

Supporting Information for:

CO₂ Absorption Enhancement Utilizing Zinc- and Cobalt-based Homogenous Catalysts

Cameron A. Lippert,^a Kun Liu,^a Moushumi Sarma,^a Sean R. Parkin,^b Joe E. Remias,^a Christine M. Brandewie,^a Guojie Qi,^a Susan A. Odom^{b*} and Kunlei Liu^{a*}

^aUniversity of Kentucky, Center for Applied Energy Research, Lexington, KY 40511-8410

^bUniversity of Kentucky, Department of Chemistry, Lexington, KY 40506-0055

E-mail: susan.odom@uky.edu, kunlei.liu@uky.edu

Table of Contents

I. Experimental Details

General Considerations

Methods and Materials

Preparation of ([IL-P]Cl), [H₂LP]Cl₂, IL-Salen(P)-Co Chloride Complex (C1P), IL-Salen(P)-Zn Chloride Complex (C3P), and IL-Salen(I)-Zn Hexafluorophosphate Complex (C3I)

Catalysts Cycle Test

Mass Transfer Measurements

Figure S1. Schematic of wetted wall column apparatus

Figure S2. Relationship of flux and driving force of CO₂

Figure S3. Schematic of CO₂ bubbling apparatus.

II. X-ray Crystallographic Data

Figure S4. Solid state structure of C3P and Selected Metrical Parameters.

Table S1. Crystallographic Data and Structure Parameters for C3P and [IL-P]Cl.

III. Carbon Loading Data

Table S2. Comparison of pH and viscosity with the addition 2.3 g/L of catalyst C1P in MEA.

Figure S5. pH values of carbon loaded samples obtained at the CAER of 5M MEA.

Figure S6. Breakthrough data of 30 wt% MEA with and without 2.3 g/L carbonic anhydrase.

Figure S7. UV-visible spectra of 0.12 mM C3I, in H₂O, with addition of 10,000 equiv. and 100,000 equiv. of sodium bicarbonate.

Figure S8. Delta-pH of C1P in 0.2 M MDEA (blue) and in the presence of 1 mol% C1P (red).

Figure S9. Carbon dioxide removal rate in 30 wt% MEA in DMSO with standard error (black), and in the presence of catalysts C1P (blue), C3I (green), and C3P (red).

Figure S10. Percent catalyst (C1P) remaining as evidenced via UV-visible spectroscopy at $\lambda_{\max} = 396$ nm while heating at 120 °C.

IV. References

I. Experimental Details

General Considerations. Routine NMR spectra were acquired on a Varian Gemini 400 spectrometer (400.392 MHz for ^1H). All chemical shifts are reported in parts per million (ppm) relative to TMS, with the residual solvent peak serving as an internal reference. UV-visible absorption spectra were acquired using a Biochrom Biowave II spectrophotometer. Unless otherwise noted, all electronic absorption spectra were recorded at ambient temperatures. All mass spectra were recorded in the University of Kentucky Mass Spectrometry Facility. Matrix-assisted laser desorption/ionization time-of-flight-mass spectrometry (MALDI-MS) was obtained using a Bruker Ultraflextreme operated in the Pos ion mode. Overall mass transfer coefficients were measured using an in-house kinetic study apparatus, wetted wall column (WWC), for gas-liquid absorption process. X-ray diffraction data was collected at 90K on either a Nonius Kappa CCD diffractometer or a Bruker-Nonius X8 Proteum diffractometer. Crystal indexing and data processing were performed either with DENZO-SMN (KappaCCD) or with Bruker APEX2 (X8 Proteum). The structures were solved with shelxs-97 and refined with shelxl-97/13. Elemental analyses were performed by Atlantic Microlab, Inc., Norcross, GA (combustion: C, H, N; flask combustion-IC: Cl) and by the Center for Applied Energy Research, Lexington, KY (ICP-MS: Zn). All analyses were performed in duplicate, and the reported compositions are the average of the two runs.

Methods and Materials. Ethanol, benzene, toluene, dichloromethane, ethyl acetate, acetone, methanol, and diethyl ether were purchased from Pharmaco-Aaper. A106 carbon steel cylinders with a total exposed surface area of 4.6 cm^2 were obtained from Metal Samples Corrosion Monitoring Systems. Nitrogen (ultra high purity) and carbon dioxide were used as received from Scott-Gross Company Inc. Deuterated DMSO (CD_3) $_2\text{SO}$ was purchased from Cambridge Isotope Laboratories and used as received. Monoethanolamine was purchased from Univar and used as received. 5-Chloromethyl-2-hydroxybenzaldehyde (5C2H), 1-(3-formyl-4-hydroxybenzyl)-3-methylimidazolium chloride ([IL-I]Cl), 1-(3-formyl-4-hydroxybenzyl)-3-methylimidazolium hexafluorophosphate ([IL-I]PF $_6$), and 1-4-hydroxy-3-[(2-[(*E*)-1-2-hydroxy-5-[(3-methyl-1H-imidazol-3-ium-1-yl)methyl]phenylmethylidene)amino]ethylimino)methyl]phenyl-3-methyl-1H-imidazol-3-ium hexafluorophosphate ([H $_2$ LI](PF $_6$) $_2$) were prepared by literature methods.¹ All characterization data matched those referenced. All other reagents were purchased from Acros Organics and used as received.

Preparation of 1-(3-Formyl-4-hydroxybenzyl)-3-triphenylphosphonium chloride ([IL-P]Cl). In a procedure adapted from literature, 5C2H (2.777 g, 16.2 mmol) and benzene (40 mL) were added to a 100 mL round-bottomed flask. Triphenylphosphine (4.577 g, 17.5 mmol) was added slowly, as a solid, with vigorous stirring. The flask was immersed in a silicon fluid bath at 80 °C and stirred for 3 h, during which a white precipitate formed. The white powder was collected via filtration through a medium porosity glass fritted funnel and washed with acetone (3 x 10 mL), yielding the product as a white solid (6.772 g, 96%). Crystals of X-ray quality were grown via slow evaporation of a solution in methanol. ^1H NMR (400 MHz, DMSO- d_6 , δ): 3.34 (s, 1H, $H_2\text{O}$); 5.11 (s, 1H, +P- CH_2); 5.15 (s, 1H, +P- CH_2); 6.98 (d, 1H, $J = 8.4\text{ Hz}$, Ar- H); 7.05 (d, 1H, $J = 8.8\text{ Hz}$, Ar- H); 7.19 (s, 1H, Ar- H); 7.7-7.87 (m, 15H, PPh_3); 10.14 (s, 1H, CHO); 11.20 (s, 1H, OH). Samples of [IL-P]Cl for elemental analysis were calculated as containing 0.5 equivalents of H_2O . H_2O is also observed in the ^1H NMR spectrum. The reported analysis is for [IL-P]Cl \cdot 0.5 H_2O . Anal. Calcd for $\text{C}_{26}\text{H}_{23}\text{ClO}_{2.5}\text{P}$: C, 70.67; H, 5.25; Found: C, 70.29; H, 5.05.

Preparation of (((1*E*,1'*E*)-(ethane-1,2-diylbis(azanylylidene))bis(methanylylidene))bis(4-hydroxy-3,1-phenylene))bis(methylene))bis(triphenylphosphonium) chloride [H $_2$ LP](Cl) $_2$. 1-(3-Formyl-4-hydroxybenzyl)triphenylphosphonium chloride (5.006 g, 11.55 mmol) and ethanol (40 mL) were added to a 100 mL round-bottomed flask. Ethylenediamine (0.40 mL, 6 mmol) was added dropwise at rt, resulting

in a yellow, homogeneous, solution. The reaction flask was immersed in a silicon oil bath at 85 °C and stirred for 3 h, then cooled to rt, after which the reaction mixture was concentrated under rotary evaporation, yielding a yellow residue. The residue was dissolved in dichloromethane (20 mL) and dropped slowly into stirring ethyl acetate (75 mL), producing a bright yellow solid. The yellow powder was collected via filtration through a medium porosity glass fritted funnel and was washed with diethyl ether (3 x 15 mL) to give the desired product as a yellow powder (4.996 g, 93%). UV-vis (DMSO) λ_{\max} , nm (ϵ , $M^{-1} \text{ cm}^{-1}$): 262 (11000), 324 (6000), 415 (1700). ^1H NMR (400 MHz, DMSO- d_6 , δ): 1.14 (t, 3H, CH_2CH_3); 1.96 (s, 3H, CH_3CO); 3.36 (br, 7H, H_2O) 3.83 (s, 4H, 2 x =N- CH_2); 4.03 (q, 2H, CH_2CH_3); 5.19 (s, 2H, +P- CH_2); 5.23 (s, 2H, +P- CH_2); 6.72 (d, 2H, J = 8.4 Hz, Ar- H); 6.90 (d, 2H, J = 8.0 Hz, Ar- H); 7.0 (s, 2H, Ar- H); 7.67-7.84 (m, 30H, PPh_3); 8.26 (s, 2H, $\text{CH}=\text{N}$). Samples of $[\text{H}_2\text{LP}](\text{Cl})_2$ for elemental analysis were calculated with 3.5 molecules of H_2O and 1 molecule of ethyl acetate. H_2O and ethyl acetate are also observed in the ^1H NMR The reported analysis is for $[\text{H}_2\text{LP}](\text{Cl})_2 \cdot 3.5 \text{ H}_2\text{O} \cdot \text{EtOAc}$, Anal. Calcd for $\text{C}_{58}\text{H}_{63}\text{Cl}_2\text{N}_2\text{O}_{7.5}\text{P}_2$: C, 66.92; H, 6.10; N, 2.69; Found: C, 67.01; H, 6.37; N, 2.99.

Preparation of $[\text{IL-Salen}(\text{P})\text{-Co}(\text{NH}_3)_2]\text{Cl}_3$ (C1P). To a 100-mL round-bottom flask was added $[\text{H}_2\text{LP}]\text{Cl}_2$ (4.594 g, 5.17 mmol), $\text{CoCl}_2 \cdot (\text{H}_2\text{O})_6$ (1.354 g, 5.69 mmol), and EtOH (40 mL) was added, producing a green-brown slurry. Ammonium hydroxide (3 mL, 35%) was added to bring the pH to 9-9.5, after which the reaction flask was immersed in a silicon fluid bath at 85 °C and stirred for 3 h, then cooled to rt after which the reaction mixture was concentrated by rotary evaporation, yielding a brown powder. The powder was washed with ice cold water to remove ammonium salts and then was triturated with ether to give the desired product as a brown powder (3.230 g, 63%). ^1H NMR (400 MHz, DMSO- d_6 , δ): 3.82 (s, 4H, 2 x =N- CH_2); 5.14 (m, 4H, 2 x +P- CH_2); 6.68 (m, 2H, Ar- H); 6.84 (t, 2H, J = 8 Hz, Ar- H); 6.97 (s, 2H, Ar- H); 7.66-7.83 (m, 30H, PPh_3); 8.25 (s, 2H, $\text{CH}=\text{N}$). ESI-MS (m/z): 963 $[\text{M-Cl}+\text{OH}_2]^+$. Samples of C1P for elemental analysis were calculated with 0.5 molecules of H_2O . H_2O is also observed in the ^1H NMR The reported analysis is for $[\text{IL-Salen}(\text{P})\text{Co}(\text{NH}_3)_2]\text{Cl}_3 \cdot 0.5 \text{ H}_2\text{O}$, Anal. Calcd for $\text{C}_{54}\text{H}_{53}\text{Cl}_3\text{CoN}_4\text{O}_{2.5}\text{P}_2$: C, 63.26; H, 5.21; N, 5.46; Cl, 10.37; Found: C, 63.19; H, 5.90; N, 5.47; Cl, 10.34.

Preparation of $\text{Zn}_2(\text{IL-Salen}(\text{P}))\text{Cl}_4$ (C3P). To a 100-mL round-bottom flask was added $[\text{H}_2\text{LP}]\text{Cl}_2$ (5.002 g, 5.63 mmol), EtOH (40 mL), and triethylamine (1.75 mL, 12.0 mmol) was added to give a clear yellow solution. Zinc chloride (1.363 g, 10.00 mmol) dissolved in EtOH (10 mL) was added, producing a pale yellow slurry. The reaction flask was immersed in a silicon fluid bath at 85 °C and was stirred for 3 h, producing a pale yellow precipitate which was collected via filtration through a medium porosity glass fritted funnel. The pale yellow powder was washed with EtOH then ether (3 x 20 mL) and air dried to give the desired product (5.679 g, 93%). Crystals of X-ray quality were grown over 5 weeks from a MeCN/EtOH/pyridine solution at 8 °C. UV-vis (DMSO) λ_{\max} , nm (ϵ , $M^{-1} \text{ cm}^{-1}$): 262 (7400), 366 (3000). ^1H NMR (400 MHz, DMSO- d_6 , δ): 3.63 (s, 2H, =N- CH_2); 3.98 (s, 2H, =N- CH_2); 6.34 (d, 1H, J = 8.0 Hz, Ar- H); 6.45 (d, J = 8 Hz, Ar- H); 6.54 (t, 1H, J = 4 Hz, Ar- H); 6.58 (dt, 1H, J = 8 Hz, J = 2.5 Hz, Ar- H); 6.68 (t, 1H, J = 4 Hz, Ar- H); 6.73 (dt, 1H, J = 8 Hz, J = 2.5 Hz, Ar- H); 7.55-7.9 (m, 30H, PPh_3); 7.97 (s, 1H, $\text{CH}=\text{N}$); 8.06 (s, 1H, $\text{CH}=\text{N}$). MALDI-MS (m/z): 555 $[\text{M}+2\text{EtOH}]^{2+}$. Samples of C3P for elemental analysis contained 2.5 molecules of H_2O . H_2O is also observed in the ^1H NMR. The reported analysis is for $\text{Zn}_2(\text{IL-Salen}(\text{P}))\text{Cl}_4 \cdot 2.5 \text{ H}_2\text{O}$, Anal. Calcd for $\text{C}_{54}\text{H}_{51}\text{Cl}_4\text{N}_2\text{O}_{4.5}\text{P}_2\text{Zn}_2$: C, 57.17; H, 4.53; N, 2.47; Zn, 11.53; Found: C, 57.05; H, 5.11; N, 2.75; Zn, 11.27.

Preparation of IL-Salen(I)-Zn Hexafluorophosphate Complex (C3I). To a 100 mL round-bottomed flask was added $[\text{H}_2\text{LI}]\text{PF}_6$ (5.011 g, 6.680 mmol), EtOH (40 mL), and triethylamine (2.0 mL, 14 mmol), which produced a yellow suspension. Zinc chloride (0.952 g, 7.00 mmol) dissolved in EtOH (10 mL) was added. The reaction flask was immersed in a silicon oil bath at 85 °C, and the yellow slurry was stirred for 4 h, producing a yellow solid which was collected via filtration through a medium porosity glass

fritted funnel. The yellow powder was washed with EtOH (3 x 30 mL), then with ether (3 x 20 mL), and was air dried to give the desired product (4.639 g, 85%). UV-vis (DMSO) λ_{max} , nm (ϵ , $\text{M}^{-1} \text{cm}^{-1}$): 263 (14100), 357 (6000). ^1H NMR (400 MHz, DMSO- d_6 , δ): 3.73 (s, 2H, =N-CH₂); 3.82 (s, 6H, CH₃); 3.93 (s, 2H, =N-CH₂); 5.20 (s, 2H, N⁺-CH₂); 5.32 (s, 2H, N⁺-CH₂); 6.89 (d, 1H, J = 8.5 Hz, ArH); 7.26 (m, 2H, ArH); 7.40 (d, 2H, J = 8.5 Hz, ArH); 7.51 (s, 1H, ArH); 7.65 (m, 4H, ArH); 8.56 (s, 1H, CH=N); 8.37 (s, 1H, CH=N); 9.11 (s, 2H, ImH). Samples for MALDI-MS were from concentrated ammonium hydroxide solutions. MALDI-MS (m/z): 537 [M+OH]⁺. Samples of **C3I** for elemental analysis contained 0.5 molecules of EtOH. EtOH is also observed in the ^1H NMR. The reported analysis is for [IL-Salen(I)-Zn]((PF₆)_{1.75}(Cl)_{0.25} • 0.5 EtOH, Anal. Calcd for C₂₇H_{31.5}Cl_{0.25}N₆O_{2.5}P_{1.75}Zn: C, 40.13; H, 3.93; N, 10.40; Zn, 8.09; Found: C, 40.03; H, 4.14; N, 10.42; Zn, 8.14.

Catalysts Cyclic Capacity Test. In a representative procedure, to a two-necked 150 mL round-bottomed flask was added 5 M aqueous MEA (25 mL) containing CAER catalyst C3I (60.0 mg, 2.3 g/L, 2.5 mM). A pH probe was immersed into the solution through one neck, and an impinger was immersed into the solution through the other neck of the flask. The solution was loaded with CO₂ by bubbling a water saturated stream of 14 vol% CO₂ gas in N₂ supplied through an MFC (Aalborg) at 0.5 L/min through the solution. Reaction progress was monitored by the change in pH over time as CO₂ was absorbed until a pH of 8.9 was obtained. The reaction vessel was fitted with a reflux condenser with circulating chilled salt water (-4 °C) and an impinger. The solution was heated at 80 °C for 75 min while N₂ gas was bubbled through the solution (~5 bubbles/sec) to remove captured CO₂, at which point the pH rose to about 10.0. The reaction vessel was again fitted with a pH probe and impinger, and a water-saturated stream of 14 vol% CO₂ gas in N₂ supplied through an MFC (Aalborg) was bubbled through the solution at 0.5 L/min. The reaction progress was again monitored by the change in pH over 900 sec with pH = 10.0 being t = 0 s. This cycle of carbon loading and heating was repeated until 5 cycles were completed.

Mass Transfer Coefficient Measurements. The wetted wall column (WWC) was setup as previously described.¹ The schematic of the WWC used in this test is shown in Extended Data Fig. 2. In a representative procedure, 30 wt% aqueous MEA is loaded to a mol CO₂/mol MEA level of approximately 0.1 with CO₂ by sparging the solution reservoir with a concentrated 30 vol% CO₂/N₂ mixture for 6-12 min. Catalyst was added to the solution (C3P, 2.3 g/L) to give a clear, yellow solution. The solution is then heated to 40 °C by circulating through a heat exchanger bath at 180 mL/min. Once the solution is thermally stable, a CO₂ gas feed mixed with N₂ at 6.6 L/min (3-14.7 vol%), pre-heated and water saturated by a direct contact heat exchanger, is allowed to contact with the liquid countercurrent on the surface of the column. Absorption or desorption of CO₂ occurs across the contacting area, which gives a CO₂ concentration difference in the gas stream between the inlet and outlet of the column. Flux and driving force can be obtained from the concentration difference. Four different CO₂ concentrations in the gas stream were tested at the same carbon loading. Liquid samples downstream of the WWC were collected during the process for carbon loading, viscosity, density, and pH measurements. The above procedure was repeated for different carbon loadings.

The overall mass transfer coefficient at the operating condition can be calculated from eq. 4.

$$K_G = \frac{N_{\text{CO}_2}}{A\Delta P_{\text{CO}_2}} \quad (4)$$

in which N_{CO_2} is the flux of CO_2 , K_G is the overall mass transfer coefficient, ΔP_{CO_2} is the log mean of CO_2 partial pressure, and A is the contacting surface area. Diffusivity of CO_2 , which is not directly measured in this work, can be calculated from a modified Stokes-Einstein equation in eq 5.

$$\left(D_{CO_2}\right)_{\text{amine soln}} = \left(D_{CO_2}\right)_{\text{water}} \left(\frac{\eta_{\text{water}}}{\eta_{\text{amine soln}}}\right)^{0.8} \quad (5)$$

in which D_{CO_2} is the diffusivity of CO_2 in amine solution or water, and η is the viscosity of amine solution or water.

The flux is calculated by the CO_2 concentration difference at the inlet and outlet of the wetted wall column as shown eq. 6.

$$N_{CO_2} = N_{CO_2}^{in} - N_{CO_2}^{out} = y_{CO_2}^{in} N_t^{in} - y_{N_2}^{in} N_t^{in} \frac{y_{CO_2}^{out}}{y_{N_2}^{out}} \quad (6)$$

in which the molar flow rates N_t were calculated from total volume flue rate at standard condition, y_i is the molar fraction of component i .

Since the CO_2 dynamically transfers from gas phase to liquid phase, the partial pressure of CO_2 decreases along the wetted wall column. To better represent the true average partial pressure of CO_2 in the column, log mean of the driving forces was taken at the inlet and the outlet of the column.

$$\Delta P_{CO_2} = \frac{P_{CO_2}^{in} - P_{CO_2}^{out}}{\ln\left(\frac{P_{CO_2}^{in} - P_{CO_2}^*}{P_{CO_2}^{out} - P_{CO_2}^*}\right)} \quad (7)$$

in which $P_{CO_2}^i$ is the partial pressure of CO_2 written as

$$P_{CO_2}^i = y_{CO_2}^i (P_{total} - P_{water}) \quad (8)$$

As the feed gas is saturated with water in the saturator, the partial pressure of water can be written as its saturation pressure at the temperature T .

$$P_{water}^i = \exp\left(72.55 - \frac{7207}{T} - 7.139 \ln(T) + 4.046 \times 10^{-6} T^2\right) \quad (9)$$

The equilibrium partial pressure of CO_2 , $P_{CO_2}^*$, can be calculated by making the flux N_{CO_2} to be zero at zero driving force through an iterative routine in MATLAB where the two equations are simultaneously solved. A typical relationship of flux N_{CO_2} and driving force of CO_2 is shown in Figure S2. The linearity of the two indicates a pseudo first order approximation.

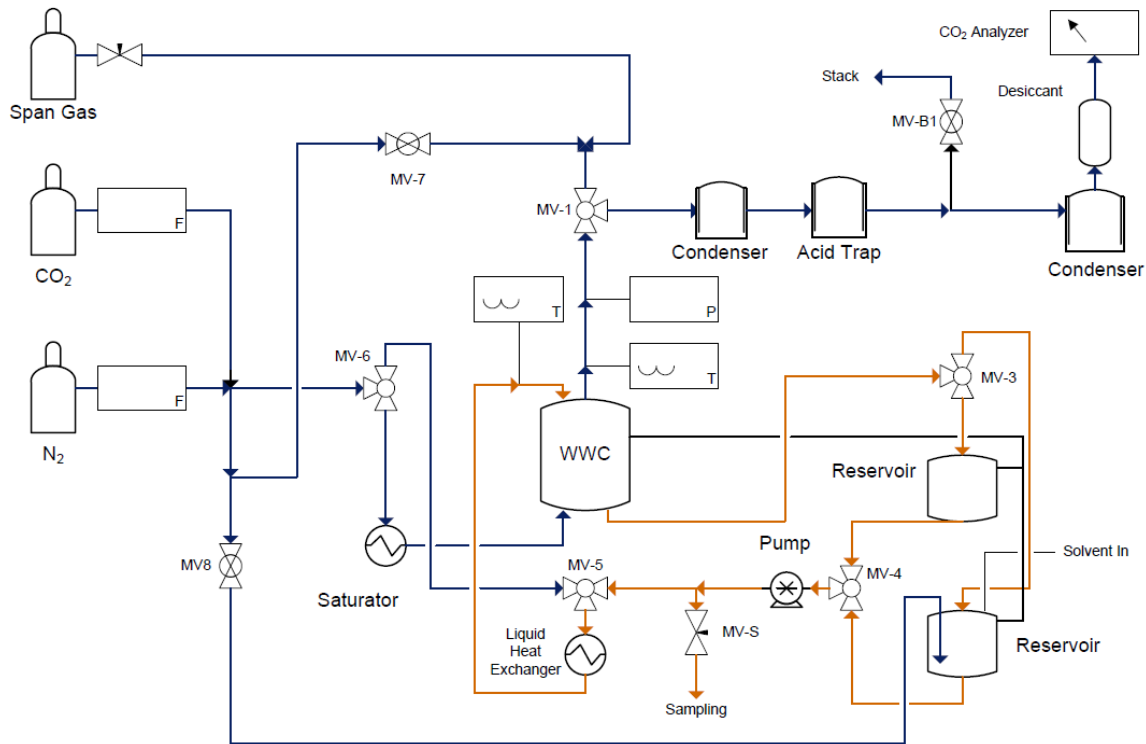


Figure S1. Schematic of wetted wall column apparatus utilized for mass transfer coefficient measurements.

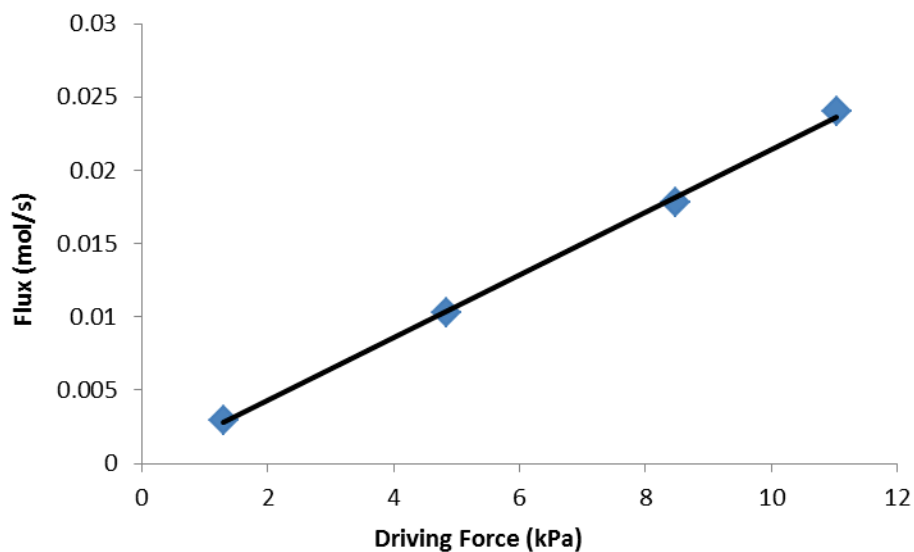


Figure S2. A typical relationship of flux N_{CO_2} and driving force of CO_2 from wetted wall column experiment.

Breakthrough Solvent Evaluation Apparatus: In a representative procedure, the breakthrough solvent evaluation apparatus consists of a 30 ml gas saturator, a 30 ml bubbler, a condenser, and a CO₂ analyzer. Both the saturator and the bubbler are made of Pyrex[®], and are immersed in a water bath maintained at 40 °C. A CO₂ feed gas stream (12%-14%) balanced with N₂ is saturated with water in the saturator and bubbled through a 30 wt% MEA solution in the bubbler (1L/min). The gas effluent is dried over drierite and analyzed for CO₂ concentration (vol%) using a CO₂ analyzer (VIA-510, HORIBA, 0.5% precision). Data of CO₂ outlet concentration with respect to time is continuously recorded with 1 second interval using an in-house Labview program.

The difference of inlet and outlet CO₂ concentration represents the absorbed amount of CO₂ at a particular time. The integration of the concentration difference represents the CO₂ loading as expressed

$$\text{CO}_2 \text{ Loading (mol CO}_2\text{/ kg solution)} = \frac{\int_0^t (C_{in} - C_{out}(t))dt}{m_{sol}}$$

in which C_{in} is the CO₂ feed gas rate in mol/s, C_{out} is the CO₂ effluent rate in mol/s, t is time in second, and m_{sol} is the mass of solution in kg.

In addition, the absorption rate can be described by the derivate of CO₂ loading with respect to time:

$$\text{Absorption rate (mol CO}_2\text{/ kg solution/s)} = \frac{d \text{ CO}_2 \text{ Loading}}{dt}$$

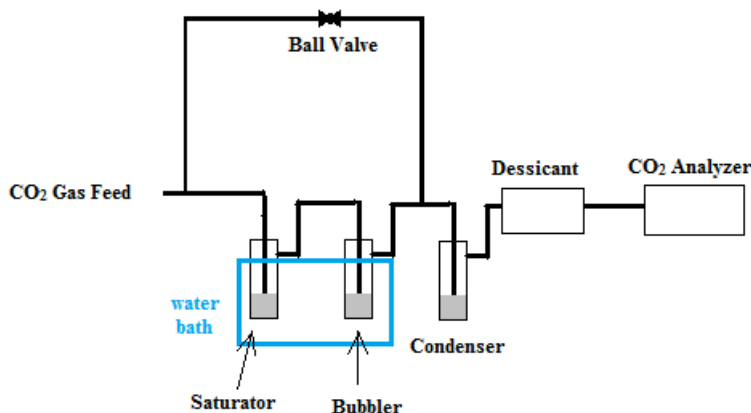


Figure S3. Schematic of simple CO₂ bubbling apparatus.

II. X-ray Crystallographic Data

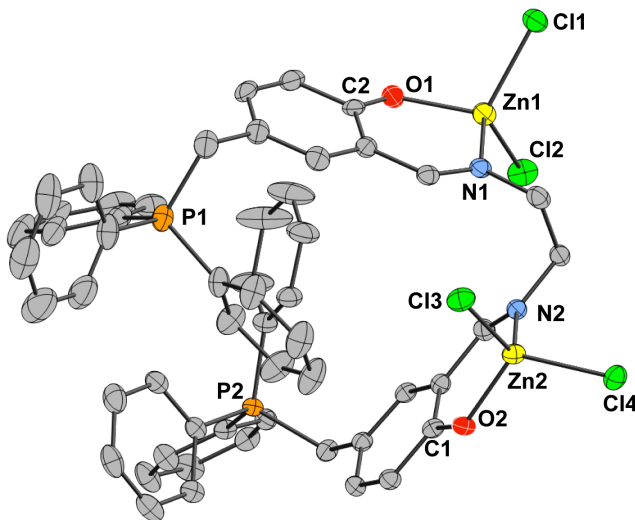


Figure S4. Solid-state structure of $\text{Zn}_2(\text{IL-Salen(P)})\text{Cl}_4$ (**C3P**) shown with 50% probability ellipsoids. Hydrogen atoms and solvents molecules omitted for clarity. Selected bond lengths (Å) and angles (deg): Zn1–O1 1.946(3), Zn1–N1 2.042(3), Zn1–Cl1 2.2431(12), Zn1–Cl2 2.616(13), Zn2–O2 1.938(3), Zn2–N2 2.043(3), Zn2–Cl3 2.317(12), Zn2–Cl4 2.442(11), O1–C2 1.282(5), O2–C1 1.304(5), O1–Zn–N1 95.47(14), O1–Zn1–Cl1 107.88(10), N1–Zn1–Cl1 113.22(10), N1–Zn1–Cl2 110.41(11), Cl1–Zn1–Cl2 113.46(5), O2–Zn2–N2 94.39(32), O2–Zn2–Cl3 111.04(9), O2–Zn2–Cl4 114.76(9), N2–Zn2–Cl3 114.21(10), N2–Zn2–Cl4 106.47(10), Cl3–Zn2–Cl4 114.32(5).

Table S1. Crystallographic Data and Structure Parameters for $[\text{Zn}^{\text{II}}_2(\text{IL-Salen(P)})\text{Cl}_4] \cdot \text{MeCN}$.

Complex	$[\text{Zn}^{\text{II}}_2(\text{IL-Salen(P)})\text{Cl}_4] \cdot \text{MeCN}$
Empirical formula	C61 H54 Cl4 N4 O2 P2 Zn2
Formula weight	1209.56
T (K)	90.0(2)
Wavelength	1.54178 Å
Crystal System	Orthorhombic
Space group	$P2_12_12_1$
Unit cell dimensions	
a (Å)	12.4064(2)
b (Å)	17.4016(3)
c (Å)	25.8891(5)
α (°)	90
β (°)	90
γ (°)	90
V (Å ³)	5589.23(17)
Z	4
D _{calc} (g cm ⁻³)	1.437
Absorption coefficient (mm ⁻¹)	3.730
Crystal size (mm)	0.120 x 0.040 x 0.030
Θ range for data collection	3.060 to 68.341
Index Ranges	$-14 \leq h \leq 6$ $-20 \leq k \leq 20$

Reflections collected/ unique	-31 ≤ l ≤ 30
Goodness-of-fit on F ²	65905/9999
R [I > 2σ(I)]	1.044
wR ₂ (all data)	0.0332
	0.0928

III. Carbon-Loading Data

Table S2. Comparison of pH and viscosity with the addition 2.3 g/L of catalyst C1P in MEA.

	30 wt% MEA	30 wt% MEA + 2.3 g/L C1P
Viscosity (cP)	1.82	1.83
pH	12.71	12.67

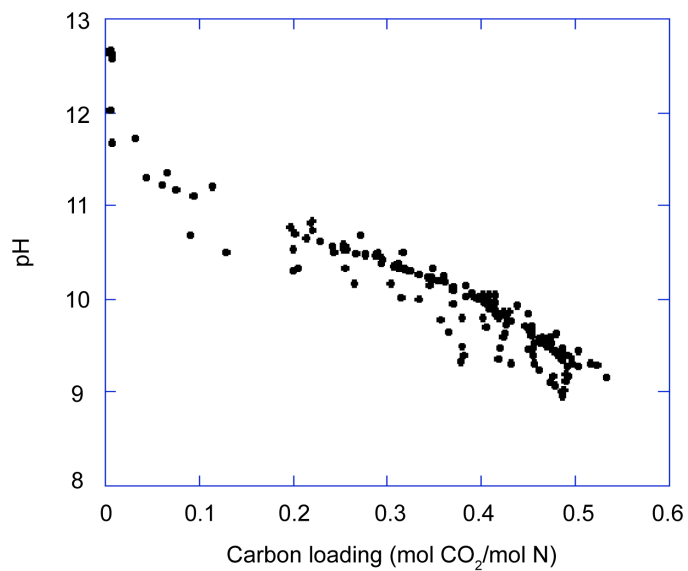


Figure S5. pH values of carbon loaded samples obtained at the CAER of 5M MEA.

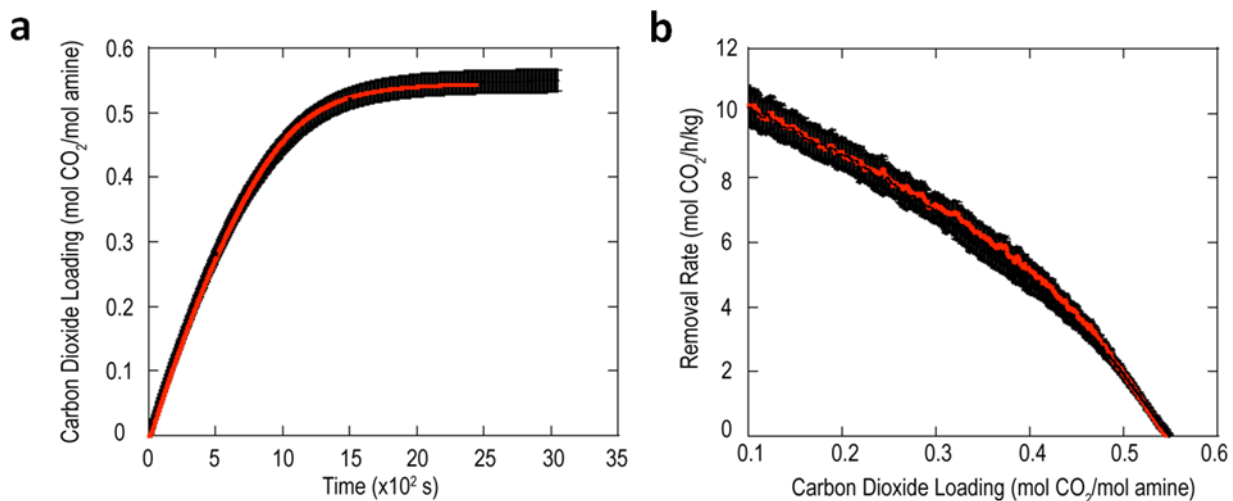


Figure S6. Breakthrough data of 30 wt% MEA with standard error of 5% (black) and 30 wt% MEA with 2.3 g/L carbonic anhydrase (red) for (a) increase in carbon loading versus time, and (b) removal rate as a function of carbon loading.

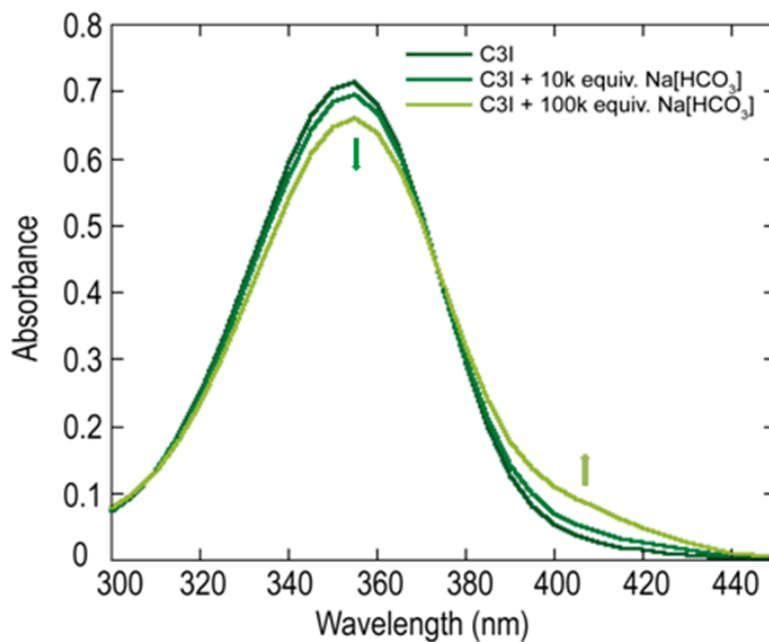


Figure S7. UV-visible spectra of 0.12 mM C3I, in H₂O, with addition of 10,000 equiv. and 100,000 equiv. of sodium bicarbonate.

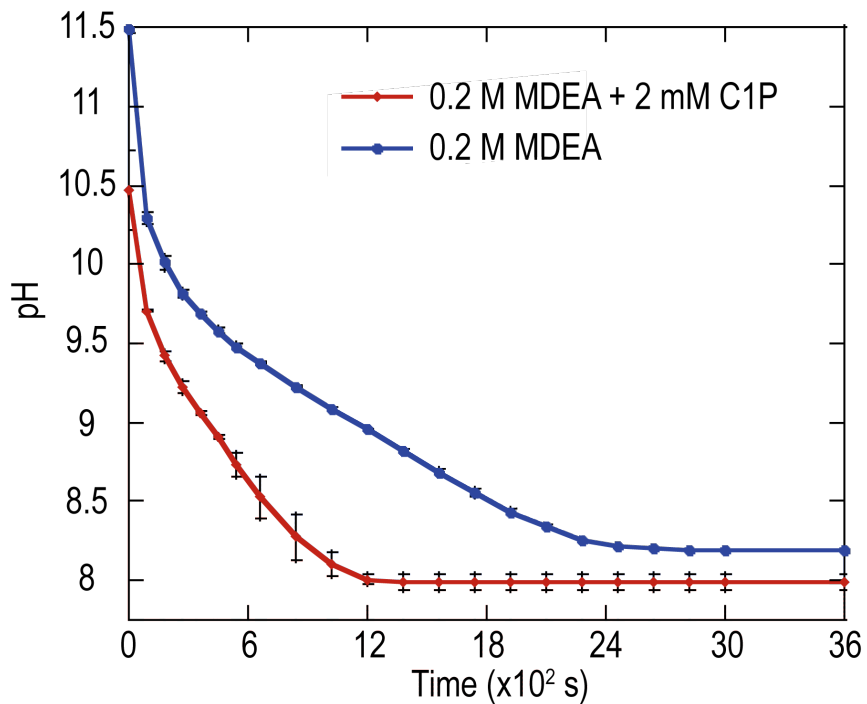


Figure S8. Delta-pH of C1P in 0.2 M MDEA (blue) and in the presence of 1 mol% C1P (red).

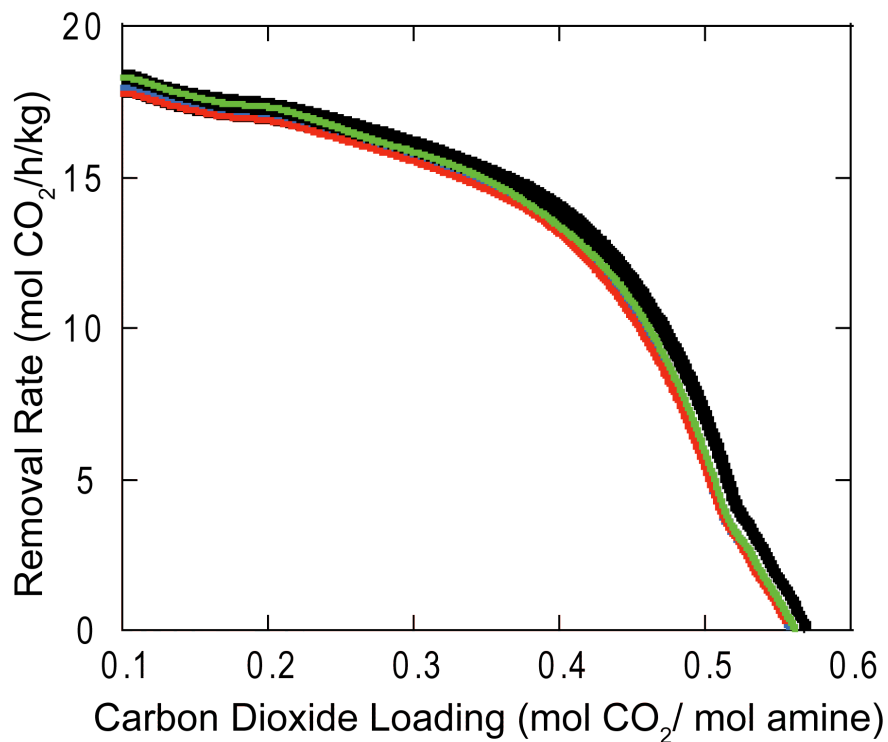


Figure S9. Carbon dioxide removal rate in 30 wt% MEA in DMSO with standard error (black), and in the presence of catalysts C1P (blue), C3I (green), and C3P (red).

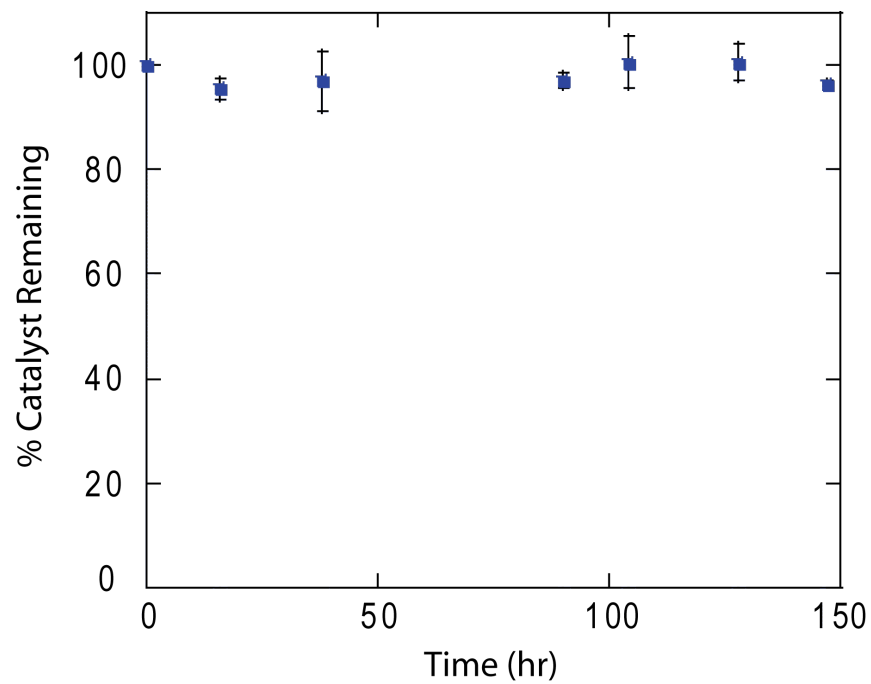


Figure S10. Percent catalyst (C1P) remaining as evidenced via UV-visible spectroscopy at $\lambda_{\text{max}} = 396$ nm while heating at 120 °C.

IV. References

(1) Liu, K.; Jinka, K. M.; Remias, J. E.; Liu, K. Absorption of Carbon Dioxide in Aqueous Morpholine Solutions, *Ind. Eng. Chem. Res.*, **2013**, 52, 45, 15932-15938.